www.amlett.com, www.amlett.org, DOI: 10.5185/amlett.2012.ib.109
"Nanostructuring by electrons, photons and ions" Special Issue Published online by the VBRI press in 2013

Swift heavy ion irradiation induced structural, optical and conformational modifications in conducting polymer nanostructures

A. Kumar[*], Somik Banerjee

Materials Research Laboratory, Dept. of Physics, Tezpur University, Tezpur 784028, Assam, India

[*] Corresponding author. E-mail: ask@tezu.ernet.in

Received: 16 March 2012, Revised: 22 July 2012 and Accepted: 26 July 2012

ABSTRACT

Structural and conformational modifications in conducting polymer nanostructures viz., Polyaniline (PAni) nanofibers induced by swift heavy ion (SHI) irradiation have been investigated employing TEM, XRD, UV-Vis, FTIR and micro-Raman spectroscopy. Upon interaction with the highly energetic ions, PAni nanofibers are fragmented and get amorphized. The local range of order is found to decrease with a corresponding increase in the concentration of point defects and dislocations leading to the enhancement in strain. Vibrational spectra of the pristine and SHI irradiated PAni nanofibers studied using FTIR and micro-Raman (μR) spectroscopy indicate conformational changes in PAni nanofibers upon SHI irradiation. Loss of π-stacking due to the enhancement in the torsion angle between C_{ring}-N-C_{ring} upon irradiation is indicative of strong electrostatic interaction between the electron rich C–N site in the aromatic rings of PAni chains and the ion beam. The most significant variation in PAni nanofibers upon SHI irradiation is the transformation of para di-substituted benzene (benzenoid) structure of PAni into the quinone di-imine (quinoid) structures; a phenomenon that has been simultaneously observed in both the FTIR and Raman spectra. The presence of two main peaks representing the same structures in PAni nanofibers in both the Raman and IR spectra is because of the presence of delocalized sp^2 phases and local disorder in PAni nanofibers, which gives rise to electrical and mechanical fluctuations that destroy the symmetry rules. Copyright © 2013 VBRI press.

Keywords: Conducting polymer; nanostructure; swift heavy ion irradiation; TEM; XRD; UV-Vis; FTIR; micro-Raman spectroscopy.

Introduction

In recent years, research in the field of conducting polymers is primarily focussed on the development of conducting polymer nanostructures, which combine the advantages of organic conductors with low dimensionality and also show better processibility. Several types of conducting polymer nanostructures such as nanofibers, nanotubes, nanoparticles, nanowires and nanoribbons have been synthesized by employing several techniques [**1-7**]. These nanostructures have applications in sensors, memory devices, microelectronics etc. [**8-10**] and in majority of the cases show better efficiency than their bulk counterpart. Polyaniline (PAni) and its derivatives are one of the most studied conducting polymers owing to their electrochromic and photoconductivity properties allied with their higher stability in air and easy doping/de-doping process, as compared to other conducting polymers [**11-13**]. Conductivity of PAni can be modified through the variation of either the number of protons, the number of electrons or both [**14**]. These properties make PAni attractive for use in solar cells, displays, lightweight battery electrodes, electromagnetic shielding devices, anticorrosion coatings and sensors [**15-18**]. Recent research efforts deal with the control and the enhancement of the bulk properties of PAni, mainly by formation of organized PAni chains in blends, composites and nanofibers. Among the PAni nanostructures, PAni nanofibers have attracted a lot of attention because of their easy synthesis, high processibility, unique applications in mesoscopic physics and fabrication of nanoscale devices. 1D nanostructures are believed to be the ideal systems for investigation of the dependence of electrical, thermal, optical and mechanical properties on quantum confinement and dimensionality [**19**]. These materials have an important impact for application in electronic devices and molecular sensors owing to their extremely high surface area, synthetic versatility and low cost [**20**]. A deep understanding and ability to control the size, shape, crystallinity and surface properties of PAni nanofibers can facilitate design and fabrication of novel devices with advanced functionalities.

Swift heavy ion (SHI) irradiation causes exotic effects in different classes of materials which otherwise cannot be generated by any other means. Ion irradiation of polymers can be used to induce irreversible modifications of their macromolecular structure, in a controlled way, leading to remarkable changes in their chemical, optical, electrical, mechanical, morphological and thermal properties [**21, 22**]. Modern technologies demand polymers with specific properties that can be achieved by using ion beams. The effects of ion‑ polymer interactions are more pronounced and quite different when they are subjected to swift heavy ions (SHI) irradiation. An energetic ion passing through a material, loses energy mainly by two nearly independent processes: (i) elastic collisions with the nuclei known as nuclear energy loss $(dE/dx)_n$, which dominates at an energy of about 1 keV/u; and (ii) inelastic collisions of the highly charged projectile ion with the atomic electrons of the matter known as electronic energy loss $(dE/dx)_e$ which dominates at an energy of about 1 MeV/u or more. Two phenomenological models viz., Coulomb-explosion model [**23**] and thermal-spike model [**24**] are generally used for explaining the transfer of electronic excitation generated by ion interaction with materials into the displacement of lattice atoms. The primary phenomena associated with the interaction of ion beam and polymers are cross-linking, chain scission and emission of atoms, molecules and molecular fragments [**25**]. The effect of high energy heavy ion irradiation on the chemical, electrical and optical properties of polymers has been investigated by several groups [**26-29**]. However, applicability of the SHI irradiation as a potential tool for tailoring the structure, size and properties of conducting polymer nanostructures has only been recently investigated by the authors [**30-32**]. In the present paper, we present a detailed study of the 90 MeV O^{7+} ion irradiation induced variations in the vibrational spectra and structure of PAni nanofibers.

Experimental

PAni nanofibers were synthesized by interfacial polymerization technique [**6**] using HCl and CSA as dopants. The synthesized nanofibers were then purified and dispersed uniformly in a 2% PVA solution for casting thin films (~30 μm) on glass slides of area 1 cm^2 for irradiation purpose. In this case PVA acts as a matrix and does not affect the properties of the PAni nanofibers. Thin films of the nanofibers were irradiated with 90 MeV O^{7+} ions with mean projected range of much larger than the thickness of the films. The irradiation fluence was varied from $3x10^{10}$ to $1x10^{12}$ ions/cm^2 using the 15UD Pelletron accelerator at the Inter University Accelerator Centre (IUAC), New Delhi. Vacuum inside the irradiation chamber was maintained with the help of a rotary and turbomolecular pump at $\sim 10^6$ torr during irradiation. The sample was irradiated at normal beam incidence. The XRD patterns of the sample before and after irradiation were acquired using a Rigaku Miniflex diffractometer with Cu K_α radiation, $\lambda = 1.5406$ Å in the 2θ range of 10‑ 70^0. A Renishaw in-Via Raman microscope with Ar ion laser (power: 0.5 mW; excitation: 514.5 nm; exposure time: 10 s) was used to acquire the micro-Raman (μR) spectra of the pristine and irradiated samples. Transmission electron micrographs were acquired using a JEOL JEM 100 CXII Transmission electron microscope (TEM).

Results and discussion

TEM micrographs of the pristine and the 90 MeV O^{7+} ion irradiated CSA doped PAni nanofibers at a fluence of 1 x 10^{12} ions/cm^2 are shown in **Fig. 1**(a, b). The variations in the diameter distribution of the PAni nanofibers are also shown as inset of the micrographs. It has been observed that PAni nanofibers undergo fragmentation and their average diameter decreases upon irradiation. The same phenomenon is observed for HCl doped PAni nanofibers and has been reported by the authors elsewhere [**30**].

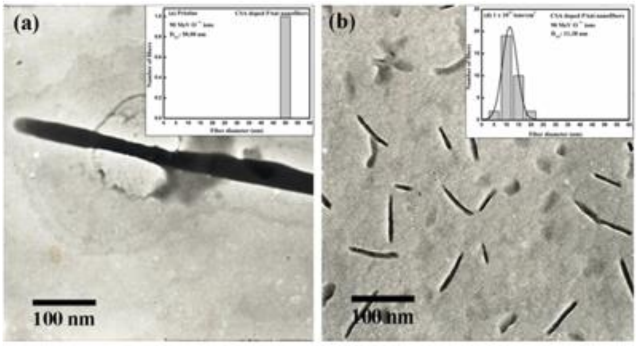

Fig. 1. Transmission electron micrographs for CSA doped PAni nanofibers (a) Pristine and (b) irradiated with 90 MeV O^{7+} ions at a fluence of 1 x 10^{12} ions/cm^2. The insets show the size distribution of the PAni nanofibers before and after irradiation.

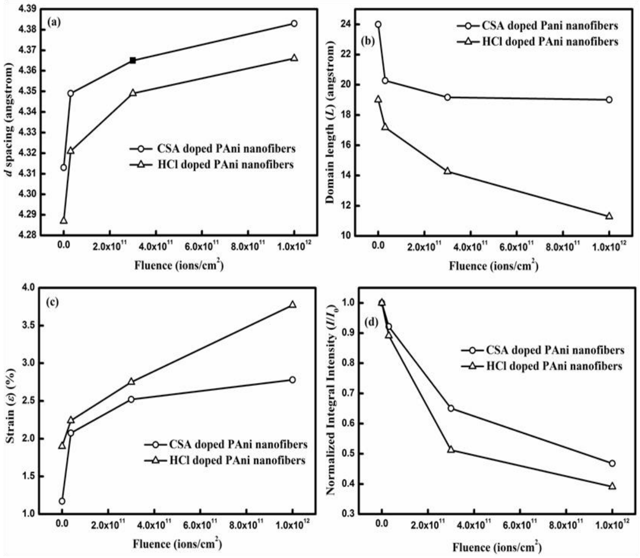

Fig. 2. Variation of (a) d-spacings, (b) domain length (L), (c) strain, and (d) normalized integral intensity of the pristine and SHI irradiated PAni nanofibers.

The authors have reported the variations in the X-ray diffraction patterns of the PAni nanofibers doped with HCl and CSA before and after SHI irradiation elsewhere [**30, 31**]. Using single line approximation, the local range of order referred to as domain length (L) in case of polymers and the strain generated in the PAni nanofibers as a result of tremendous electronic energy deposition upon irradiation have been calculated. Figs. 2 (a-d) show the variations of the d-spacings, domain length (L), strain (ε), and the normalized integral intensity (I/I_0) of the PAni nanofibers as a function of irradiation fluence. The decrease in domain length (*L*) with increasing fluence [**Fig. 2b**] can be interpreted as a decrease in the crystalline domain size accompanied by a reduction in the Cl/N ratio upon SHI irradiation [**33**]. The increase in the strain in the material with increasing irradiation fluence may be attributed to the creation of point defects and dislocations due to the tremendous amount of electronic energy deposition in the material. Furthermore, the increase in *d*-spacing with increasing ion fluence indicates an increase in the angle at which the chains tilt with respect to the (*a*, *b*) basal plane of polyaniline. The increase in the *d*-spacings may also be interpreted as a reduction in π-stacking and a corresponding decrease in the Cl/N ratio [**33**]. The amorphization of the material upon SHI irradiation is confirmed by the decrease in the normalized integral intensity (I/I_0) [**Fig. 2d**].

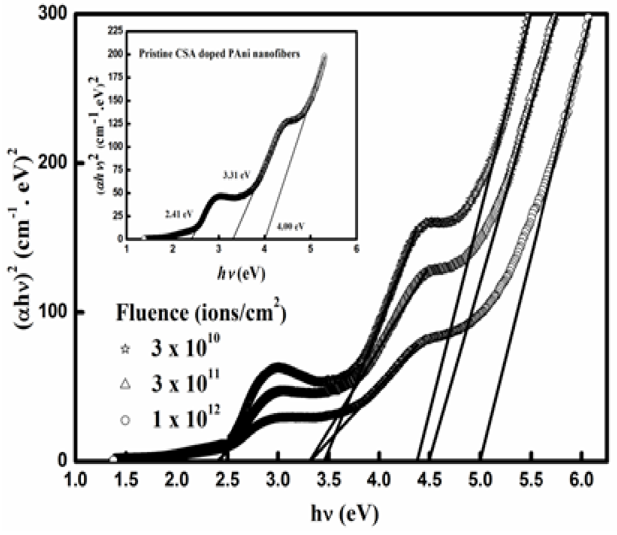

Fig. 3. $(\alpha h\nu)^2$ vs. $h\nu$ plots for the pristine and irradiated CSA doped PAni nanofibers

Fig. 3 shows the plot of $(\alpha h\nu)^2$ vs. $h\nu$ for the CSA doped PAni nanofibers irradiated with 90 MeV O^{7+} ions at different fluences viz., 3 x 10^{10}, 3 x 10^{11} and 1 x 10^{12} ions/cm^2. The inset of the **Fig. 3** shows the $(\alpha h\nu)^2$ vs. $h\nu$ plots for the pristine CSA doped PAni nanofibers. The optical transitions in PAni nanofibers have been found to be of the allowed direct type [**32**]. The direct optical band gaps for the pristine and irradiated samples have been determined from the plot of $(\alpha h\nu)^2$ vs. photon energy $h\nu$. It has been observed from **Fig. 3** that the direct optical band gap of the material increases with increasing irradiation fluence. This increase in the direct optical band gap values can be attributed to two factors: (i) the fragmentation of the PAni nanofibers upon SHI irradiation as observed from TEM micrographs and (ii) a decrease in the extent of conjugation which suggests that the adjacent phenyl rings of the polymer have larger torsion angles with respect to the plane of the nitrogen atoms.

Vibrational spectroscopy is an important tool for studying the conformational variations, structure and short range order in polyaniline (PAni) [**34-36**]. **Fig.**s 4(a, b) show the FTIR and the micro-Raman (μR) spectra of the CSA doped PAni nanofibers before and after 90 MeV O^{7+} ion irradiation. In **Fig.** 4(a), the vibrational band at 1670 cm^{-1} occur due to the N–H bending while the band at 3300 cm^{-1} may be assigned to the N-H stretching of the benzenoid units of the emeraldine form of PAni. The peaks at 1400 cm^{-1} and 1460 cm^{-1} are assigned to the C=C stretching vibrations of the para di-substituted benzene (benzenoid) and the quinone di-imine (quinoid) units of PAni, respectively. The band at 1199 cm^{-1} is ascribed to the C–N bending vibration mode. The band at 1122 cm^{-1} has been ascribed to the C–H in plane deformation while the peaks at 600 and 660 cm^{-1} are assigned to the C–H out of plane deformations of the mono-substituted and para di-substituted benzene rings.

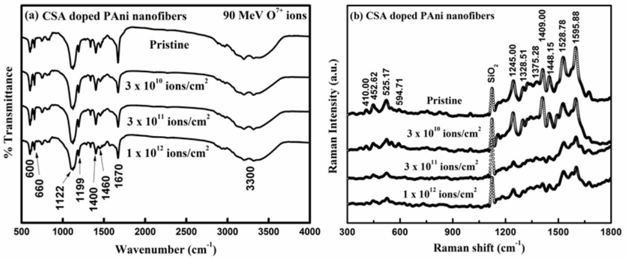

Fig. 4. (a) Vibrational bands in pristine and SHI irradiated CSA doped PAni nanofibers (a) FTIR spectra showing IR active vibration modes and (b) Micro-Raman showing Raman active modes.

Fig. 4(b) shows the μR spectra of the pristine and irradiated PAni nanofibers doped with CSA obtained with Ar ion laser of 0.5 mW power and 514.5 nm excitation. In the μ-Raman spectra of the pristine PAni nanofibers, the C–H benzene deformation modes at 1182.63 cm^{-1} indicate the presence of quinoid rings. The bands at 1451.30 and 1417.18 cm^{-1} correspond to the C=N stretching mode of the quinoid units. The band at 1248.11 cm^{-1} can be assigned to the C–N stretching mode of the polaronic units. The absorption band at 1375.28 cm^{-1} corresponds to the C–N$^+$ stretching modes of the delocalized polaronic charge carrier, which indicates that the PAni nanofibers are in doped ES-I form. The band at 1328.51 cm^{-1} is a characteristic of the semiquinone radical cation. The absorption peak at 1528.78 cm^{-1} corresponds to the N–H bending deformation band of protonated amine. The C-C deformation band of the para di-substituted benzene rings is positioned at 1595.88 cm^{-1}.

All the prominent vibrational bands of PAni nanofibers as observed from the FTIR and Raman spectra show a decrease in intensity which indicates that SHI irradiation induces amorphization of the material. This fact is supported by the domain length (*L*) of the irradiated PAni nanofibers determined using X-ray diffraction analysis upon SHI irradiation. The decrease in intensity of the Raman active modes at 1248.11 and 1375.28 cm^{-1} due to the polaronic charge carriers indicate that PAni nanofibers also get dedoped upon SHI irradiation. The decrease in the intensity of the Raman active modes in the low wave number region indicate changes in the crystallinity arrangement of the PAni nanofibers, specifically increase of the torsion angles of the C_{ring}–N–C_{ring} segments [**37, 38**]. This increase in the torsion angles is due to the loss of π-stacking among the PAni rings, leading to amorphization of the nanofibers, which is also corroborated by the XRD results. The results indicate that the electronic interaction between the electron rich C–N site in the aromatic rings of

PAni chains and the ion beam might have induced distortion of the polymeric chains leading to conformational modifications of the PAni nanofibers.

The most significant variation in the vibrational spectra of PAni nanofibers can be observed in the C=C stretching vibration mode of the para di-substituted benzene (benzenoid) and quinine di-imine (quinoid) structures. **Fig. 5**(a, b) shows the deconvolution of the sub-peaks representing C=C stretching of the benzenoid and the quinoid resonant structures in the FTIR and Raman spectra for the pristine and irradiated samples. In the FTIR spectra [**Fig. 5**(a)], the intensity of the peak at 1400 cm^{-1} due to the C=C stretching of the benzenoid ring of PAni nanofibers decreases with the increase in ion fluence, whereas the C=C stretching vibration for the quinoid structure shows an increase in intensity. In the Raman spectra of the pristine and irradiated PAni nanofibers [**Fig. 5**(b)], it can be seen that the C-C stretching vibrations of the para di-substituted benzene ring can be deconvoluted into two sub peaks. The sub-peaks indicate two kinds of resonant structures: the main peak is due to the para di-substituted benzene (benzenoid) structure and the shoulder peak is due to the quinone di-imine (quinoid) structure of the PAni nanofibers. As the fluence of SHI irradiation increases the main peak of the symmetric C=C stretching mode is up-shifted [**Fig. 5**(b)] and the intensity decreases. The shoulder peak of the symmetric C=C stretching mode is also up-shifted but the intensity of the peak increases more than three times upon SHI irradiation.

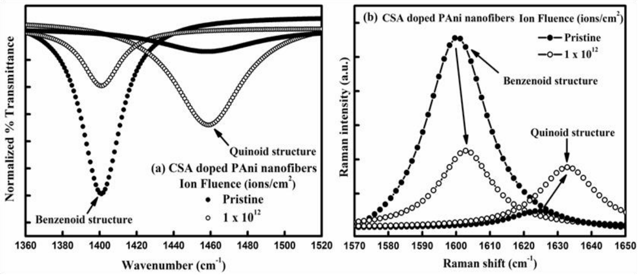

Fig. 5. Comparison of the deconvoluted sub-peaks representing the C=C stretching due two the para di-substituted benzene (benzenoid) rings and the quinone di-imine (quinoid) rings for the pristine and irradiated PAni nanofibers from (a) FTIR spectra and (b) Micro-Raman spectra.

Both the FTIR and the Raman spectra point out to the fact that the intercyclic rings of the PAni nanofibers become distorted upon SHI irradiation; the proportion of the para di-substituted benzene rings (benzenoid) decreases, while there is a corresponding increase in that of the quinone di-imine rings (quinoid) upon SHI irradiation. It is, however, interesting to note that both FTIR and Raman spectra of PAni exhibit peaks which bear the signatures of para di-substituted benzene (benzenoid) and the quinone di-imine (quinoid) structures, which is the main point of discussion in the present paper.

Inelastic light scattering from condensed matter is due to fluctuations of the dielectric susceptibility which, in turn, is related to the spectrum of dynamic excitations of the system. In crystals, momentum conservation during the scattering event only allows zone-center phonons to be Raman-active while acoustic modes are inactive. Structure disorder such as stacking fault induces the Brillouin zone folding; hence, some optical phonons become active [**39**]. These restrictions are removed in amorphous solids, and all modes could be active. Essentially it is the local disorder of amorphous materials which leads to the electrical and mechanical fluctuations. These fluctuations destroy the symmetry rules which account for the acoustic Raman active modes.

Doping induces very intense Infra-Red (IR) bands, which was ascribed to mysterious Raman active modes, however, it was shown later that the new modes arise from the breakdown of the electrical symmetry by the removal or injection of charges [**39**]. The intensity of the IR modes is due to the very large charge fluxes and a longer conjugation length. The modes with high IR intensity tend to have the highest electron phonon coupling. The vibrations giving rise to the maximum electron-phonon coupling are also the ones responsible for the highest Raman intensity modes in the undoped conjugated materials [**39-40**]. Only in the case of conjugated molecules terminated by a donor (D) and acceptor (A) groups forming a D-π-A system, the intra-molecular charge transfer creates a strong link between IR and Raman active modes. In the present case, the most prominent features in the Raman spectrum are also strongly active in the IR [**40**].

Raman scattering is a resonant process, so that the spectral line shapes change with varying excitation energy. This depicts that the similarity between the FTIR and Raman spectra taken at visible excitation is purely accidental. However, the apparent similarity between the Raman and IR spectra, in particular, the presence of two main peaks representing the same structures in PAni nanofibers can be explained as follows: Raman spectrum at a given excitation energy weights those configurations resonant with that energy. Thus Raman spectra excited with lower IR photons resonate with the most delocalized sp^2 phases, with the lowest gap. Therefore, it can be assumed that the IR spectra and the Raman spectra excited in limit of low energy will probe the same sp^2 structures. Thus, the transition of the para di-substituted benzene (benzenoid) structure to the quinone di-imine (quinoid) structure in PAni nanofibers upon SHI irradiation can be probed by the IR as well as Raman spectroscopy.

Conclusion

In summary, we have investigated the SHI induced structural, optical and conformational changes in conducting polymer nanostructures by means of TEM, XRD, UV-Vis, FTIR and micro-Raman spectroscopy. XRD analysis shows that as the irradiation fluence increases, the crystalline domain size decreases while the strain increases. The decrease in the integral intensity for the (100) peak indicate that the PAni nanofibers are amorphized upon SHI irradiation. The optical band-gap of the PAni nanofibers increases with increasing irradiation fluence. Conformational modifications in the PAni nanofibers upon SHI irradiation have been mapped using FTIR and micro-Raman spectroscopy. Both the spectra indicate a transformation from the benzenoid to quinoid structures in PAni nanofibers upon SHI irradiation. The fact that the vibrational mode representing the same structural configurations are probed by both FTIR and Raman spectra is primarily because of the delocalized sp^2 conjugated structure of the amorphous PAni nanofibers and the local disorders in these amorphous materials that lead to the breakdown of the symmetry rules.

Acknowledgements

The authors would like to sincerely thank Dr. D. K. Avasthi for useful discussions. The pelletron staff of IUAC, New Delhi and the staff of the Electron microscopy division, SAIF, NEHU, Shillong is highly acknowledged.

Reference

1. Zhang, X.; Manohar, S. K. *Chem. Commun.* **2004**, *20*, 2360
DOI: 10.1039/B409309G
2. Qiu, H.; Zhai, J.; Li, S.; Jiang, L.; Wan, M. *Adv. Funct. Mater.* **2003**, *13*, 925
DOI: 10.1002/adfm.200304366
3. Wei, Z.; Wan, M.; Lin, T.; Dai, L. *Adv. Mater.* **2003**, *15*, 136
DOI: 10.1002/adma.200390027
4. Zhang, L.; Wan, M. *Nanotechnology* **2002,** *13*, 750
DOI:10.1088/0957-4484/13/6/311
5. Wei, Z.; Zhang, Z.; Wan, M. *Langmuir* **2002**, *18*, 917
DOI: 10.1021/la0155799
6. Huang, J.; Kaner, R.B. *J. Am. Chem. Soc.* **2004**, *126*, 851
DOI: 10.1021/ja0371754
7. Pinto, N. J.; Ramosa, I.; Rojas, R.; Wang, P. –C.; Johnson, A. T. *Sens. Actuators B* **2008,** *129*, 621
DOI:10.1016/j.snb.2007.09.040
8. Han, G.; Shi, G. *Sens. Actuators B* **2004**, *99*, 525
DOI:10.1016/j.snb.2004.01.001
9. Pernaut, J. M-.; Reynolds, J. R.; *J. Phys. Chem B* **2000**, *104*, 4080
DOI: 10.1021/jp994274o
10. Virji, S.; Huang, J.; Kaner, R. B.; Weiller, B. H.; *Nano. Lett.* **2004**, *4*, 491
DOI: 10.1021/nl035122e
11. MacDiarmid, A. G.; Epstein, A. J. *Faraday Discuss: Chem. Soc.*, **1989**, *88*, 317
DOI: 10.1039/DC9898800317
12. Genies, E. M.; Boyle, A.; Lapkowski, M.; Tsintavis, C.; *Synth. Met.* **1990**, *36*, 139
DOI: 10.1016/0379-6779(90)90050-U
13. MacDiarmid, A. G. *Synth. Met.* **2002**, *125*, 11
DOI: 10.1016/S0379-6779(01)00508-2
14. Huang, W. S.; Humphrey, B. D.; MacDiarmid, A. G. *J. Chem. Soc. Faraday Trans. 1.* **1986**, *82*, 2385.
DOI: 10.1039/F19868202385
15. Carswell, A. D. W.; O'Rear, E. A.; Grady, B. P. *J. Am. Chem. Soc.* **2003**, *125*, 14793
DOI: 10.1021/ja0365983
16. Yeh, J. M.; Liou, S. J.; Lai, C. Y.; Wu, P. C. *Chem. Mater.* **2001**, *13*, 1131
DOI: 10.1021/cm000938r
17. Ogurtsov, N. A.; Pud, A. A.; Kamarchik, P.; Shapoval, G. S. *Synth. Met.* **2004**, *143*, 43
DOI: 10.1016/j.synthmet.2003.10.015
18. Jureviciute, I.; Brazdziuviene, K.; Bernotaite, L.; Šalkus, B.; Malinauskas, A. *Sens. Actuators B* **2005**, *107*, 716
DOI: 10.1016/j.snb.2004.11.075
19. Xia, Y.; Yang, P.; Sun, Y.; Wu, Y.; Mayers, B., Gates, B., Yin, Y.; Kim, F.; Yan, H. *Adv. Mater.* **2003**, *15*, 353
DOI: 10.1002/adma.200390087
20. Cardin, D.J. *Adv. Mater.* **2002**, *14*, 553
DOI:10.1002/1521-4095(20020418)14:8<553::AID-ADMA553>3.0.CO;2-F
21. Bouffard, S.; Gervais, B.; Leroy, C. *Nucl. Instrum. Methods B* **1995**, 105, 1
DOI: 10.1016/0168-583X(95)00525-0
22. Tripathi, A.; Kumar, A.; Singh, F.; Kabiraj, D.; Avasthi, D. K.; Pivin, J. C. *Nucl. Instrum. Methods B* **2005**, 236, 186
DOI:10.1016/j.nimb.2005.04.059
23. Bringa E. M.; Johnson, R. E. *Phys. Rev. Lett.* **2002**, *88*, 165501
DOI: 10.1103/PhysRevLett.88.165501
24. Wang, Z.G.; Dufour, C.; Paumier, E.; Toulemonde, M. *J. Phys.: Condens. Matter* **1994**, *6*, 6733
DOI: 10.1088/0953-8984/6/34/006
25. Davenas, J.; Boiteux, G.; Xu, X. L.; Adem, E. *Nucl. Instr. and Meth B* **1988**, *32*, 136
DOI: 10.1016/0168-583X(88)90196-6
26. Hussain, A. M. P.; Saikia, D.; Singh, F.; Avasthi, D. K.; Kumar, A. *Nucl. Instrum. Meth. B* **2005**, *240*, 834
DOI: 10.1016/j.nimb.2005.06.204
27. Hussain, A. M. P.; Kumar, A.; Saikia, D.; Singh, F.; Avasthi, D. K.; *Nucl. Instrum. Meth. B* **2005**, *240*, 871
DOI:10.1016/j.nimb.2005.06.211
28. Virk, H. S.; Chandi, P. S.; Srivastava, A. K. *Nucl. Instrum. Meth. B* **2001**, 183, 329
DOI: 10.1016/S0168-583X(01)00743-1
29. Virk, H. S.; *Nucl. Instrum. Meth. B* **2002**, 191, 739
DOI: 10.1016/S0168-583X(02)00644-4
30. Banerjee, S.; Saikia, J. P.; Kumar, A.; Konwar, B. K. *Nanotechnology* **2010**, *21*, 45101
DOI: 10.1088/0957-4484/21/17/175102
31. S. Banerjee, A. Kumar, *Nucl. Instrum. Meth. B* **2010**, *268*, 2683
DOI: 10.1016/j.nimb.2010.06.003
32. S. Banerjee, A. Kumar, *Nucl. Instrum. Meth. B* **2011**, *269*, 2798
DOI: 10.1016/j.nimb.2011.09.004
33. Pouget, J. P.; Jozefowicz, M. E.; Epstein, A. J.; Tang, X.; MacDiarmid, A. G. *Macromolecules* **1991**, *24*, 779
DOI: 10.1021/ma00003a022
34. Furukawa, Y.; Ueda, F.; Hyodo, Y.; Harada, I.; Nakajima, T.; Kawagoe, T. *Macromolecules* **1988**, *21*, 1297
DOI: 10.1021/ma00183a020
35. Colomban, Ph.; Folch, S.; Gruger, A. *Macromolecules* **1999**, *32*, 3080
DOI: 10.1021/ma981018l
36. Nascimento, G. Kobata, P. Y. J.; Temperini, M. L. A.; *J. Phys. Chem. B* **2008**, *112*, 11551
DOI: 10.1021/jp804154k
37. Cochet, M.; Louarn, G.; Quillard, S.; Boyer, M. I.; Buisson, J. P.; Lefrant, S.; *J. Raman Spectrosc.* **2000**, *31*, 1029
DOI:10.1002/1097-4555(200011)31:11<1029::AID-JRS640>3.0.CO;2-A
38. Cochet, M., Louarn, G.; Quillard, S.; Buisson, J. P.; Lefrant, S. *J. Raman Spectrosc.* **2000**, *31*, 1041
DOI:10.1002/1097-4555(200012)31:12<1041::AID-JRS641>3.0.CO;2-R
39. Ehrenfreund, E.; Vardeny, Z.; Brafman, O.; Horowitz, B. *Phys. Rev. B* **1987**, *36*, 1535
DOI: 10.1103/PhysRevB.36.1535
40. Del Zoppo, M.; Tommasini, M.; Castiglioni, C.; Zerbi, G. *Chem. Phys. Lett.* **1998**, *287*, 100
DOI: 10.1016/S0009-2614(98)00150-X